



Numerical simulation investigations of coalbed methane drainage performance with multilateral well

Songze Liu¹ · Jianguang Wei^{1,2} · Yuanyuan Ma¹ · Hongliang Liu³ · Xuemei Liu⁴ · Bingxu Yan⁵

Received: 30 October 2020 / Accepted: 1 February 2021 / Published online: 7 March 2021
© The Author(s) 2021

Abstract

A novel multilateral well for coalbed methane extraction was proposed in the study. There is a main wellbore at the longitudinal center of coal seam and four lateral wells at the horizontal center in the multilateral-well system. Compared with traditional drainage holes, multilateral-well system has a better performance on coalbed methane development. A hydraulic-mechanical coupling model of multilateral well was established, the pressure and permeability ratio distribution of the gas extraction process were analyzed comprehensively. The sensitivity analysis of lateral number, length distribution and intersection angle of multilateral-well system were studied. The results indicate that there is a minimum gas pressure distribution around the multilateral well and the overall permeability of coal seams increases with production time and the permeability around the multilateral well is larger than the area away from the multilateral well which induced by the gas desorb and matrix shrink. The quantity of lateral wells has a positive effect on cumulative production. When the total length of lateral wells is equal, the uniformity and symmetry of lateral length distribution are two key factors on the gas extraction performance. The minimum intersection angle has a positive effect on cumulative production. This study provides a better alternative for traditional drainage hole to obtain greater coalbed methane performance.

Keywords Numerical simulation · Multilateral well · Hydraulic-Mechanical coupling · Sensitivity analysis · Gas extraction performance

Introduction

The development and utilization of clean resources has long been a question of great interest worldwide (Uddin et al. 2015; Prabu and Mallick 2015; Luo et al. 2011; Chen et al. 2019a; Ma et al. 2020a, 2020b). As an important component of clean resources, coalbed methane (CBM) has become an important part of energy supply (Fan et al. 2019; Wang et al. 2018; Fan and Liu 2018; Feng et al. 2018; Yu and Wang 2020; Talapatra 2020). China's CBM resources within a buried depth of 2000 m can reach $36.8 \times 10^{12} \text{ m}^3$ and China has over 40 years' experience in CBM development (Mu et al. 2015; Luo et al. 2019; Xu et al. 2019). China has drilled about 20,000 CBM wells by 2015, but only a quarter of them were capable of mining gas commercially (Yan et al. 2019; Li et al. 2015). Achieving high efficiency and high yield of CBM wells has always been a key issue for scholars at home and abroad (Li et al. 2019; Wei et al. 2019a; Sun et al. 2019; Qin et al. 2018; Mohammed et al. 2020; Xiong et al. 2020; Talapatra and Karim 2020).

✉ Jianguang Wei
3106097170@qq.com

✉ Yuanyuan Ma
mayuanyuan_1991@outlook.com

¹ Department of Petroleum Engineering, Northeast Petroleum University, Heilongjiang Province, Daqing 163318, China

² Key Laboratory of Continental Shale Hydrocarbon Accumulation and Efficient Development (Northeast Petroleum University), Ministry of Education, Daqing 163318, China

³ PetroChina Changqing Oilfield No. 1 Oil Production Plant, Yanan 716000, China

⁴ PetroChina Daqing Oilfield No. 1 Oil Production Plant, Daqing 163318, China

⁵ PetroChina Tarim Oilfield Dina Oil and Gas Development Department, Kuerle 841000, China

The well is the key issue for the highly efficient development of CBM reservoirs (Wei et al. 2019b; Yang et al. 2017; Chen et al. 2019b; Moore et al. 2015). Zhang (Zhang et al. 2018) conducted gas drainage experiments to optimize the borehole length; the results shows that longer boreholes resulted in higher gas production and the relationship between gas production and bore hole length is a logarithmic function. Liu (Liu et al. 2013) optimized the drainage parameters of CBM wells in southern Qinshui Basin of China and the results indicated that the maximum wellhead pressure should be maintained around 1.5 MPa before stable production, and between 0.10 MPa and 0.30 MPa after stable production. Liu (Liu et al. 2018) also analyzed the inter-well interference during multi-well drainage in CBM production areas and found that the inter-well interference during multi-well drainage increases and then begins to stabilize, established geochemical response model and evaluation program of inter-well interference. Shi (Shi et al. 2019) established the pressure propagation model for vertically fractured CBM wells and vertical CBM wells without fracturing under the condition of considering variable mass flow within hydraulic fracture and hydraulic fracture conductivity decrease; the results showed that the cumulative gas production of CBM wells (CGPC) decreases sharply when permeability is less than 0.5 mD. Yang (Yang et al. 2018) developed a semi-analytical model to predict gas and water production in CBM reservoirs with multiscale fracture networks and the model was applied to quantify the effects of fracture network complexity, connectivity and stress sensitivity on extraction performance. An (An et al. 2015) compared the CBM mining performance of horizontal producer parallel to butt cleats and the alternative well configuration where the orientation of horizontal producers is parallel to face cleats; the results indicated that the former well configuration the producers can intersect the maximum number of

high-permeability pathways. Vishal (Vishal et al. 2013) designed one CO₂ injector well and two methane producer wells for CBM development and found that the methane production is significantly enhanced due to injection of CO₂.

Previous studies mainly focused on the vertical wells, horizontal wells and drainage holes in CBM reservoir, there is a deficiency investigation on the application of multilateral wells in CBM reservoir. Therefore, this study proposed a novel multilateral well for coalbed methane development. In the multilateral-well system, there is a main wellbore at the longitudinal center of coal seam and four lateral wells at the horizontal center as shown in Fig. 1. A hydraulic-mechanical coupling model was established for the novel multilateral-well system. Based on the model, the pressure distribution and permeability distribution of the gas extraction process with multilateral well were analyzed comprehensively. The gas extraction performance with multilateral well and drainage holes were compared; the sensitivity analysis of lateral number, length distribution and intersection angle of multilateral well system were studied.

Model description

Model assumptions

This study set out to investigate the gas extraction performance in coal seam with multilateral well. In order to analyze the process of coalbed methane extraction clearly, some unimportant factors have been eliminated. The following major assumptions are made to establish the numerical model (Liu et al. 2017a, 2017b, 2017c): (1) the coal seam is regarded as an idealized porous media with properties of homogeneous and isotropic; (2) the gas migration is single-phase flow and the process can be described by Darcy's Law; (3) the gas desorption process conforms to the Langmuir equation; (4) The temperature of coal seam is assumed to be constant and neglects the effect of temperature on gas

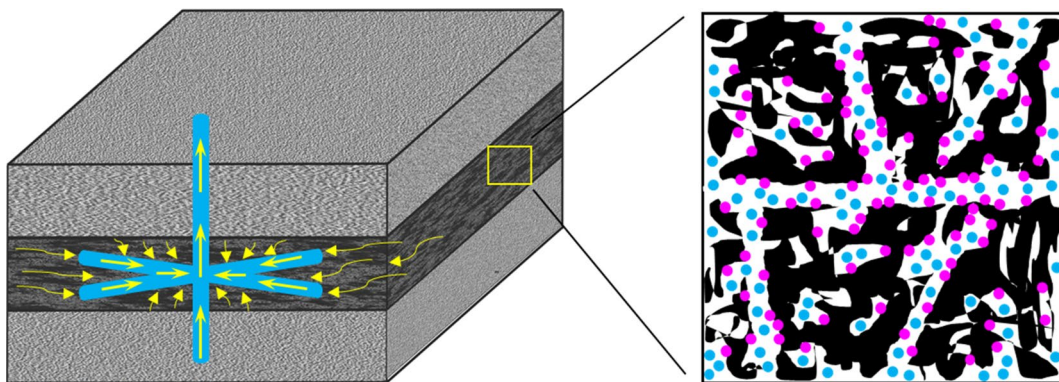


Fig. 1 Schematic of multilateral well in coal seams

desorption; (5) No flow boundary condition is set around the coal seam, the coal is saturated with gas and ignores the effect of water on gas migration; (6) the gas volume force is not considered.

Governing equation

Seepage governing equation

The mass conservation equation of gas migration in coal seams can be expressed as follows

$$\nabla(\rho_g u_g) + \frac{\partial C}{\partial t} = 0, \quad (1)$$

where ρ_g (kg/m³) is the gas density, u_g (m/s) is the gas seepage velocity, C (kg/m³) is the gas content in coal seams and t (s) denotes the time. The gas seepage velocity u_g can be described by Darcy's Law

$$u_g = -\frac{k}{\mu} \nabla p_g, \quad (2)$$

where p_g (Pa) is the gas pressure, k (m²) is the effective permeability of the coal seams and μ (Pa · s) is the gas dynamic viscosity. The gas content C in coal seams is written as follows

$$C = C_a + C_f \quad (3)$$

$$C_a = \frac{p_g ab}{1 + bp_g} \rho_c \rho_g \quad (4)$$

$$C_f = \varphi \rho_g, \quad (5)$$

where C_a (kg/m³) and C_f (kg/m³) represent adsorption gas content and free gas content, φ and ρ_c (kg/m³) represent the porosity and density of coal seams, a and b represent Langmuir adsorption constant and pressure constant, respectively. The parameter ρ_g can be calculated by the modified ideal gas state equation as follows

$$\rho_g = \frac{M p_g}{RT Z}, \quad (6)$$

where M (kg/mol) is the gas molar mass, R (8.314 J/(K · mol)) is the ideal gas constant, T (K) is the ambient temperature and Z is the gas compression factor. Substituting Eqs. (2), (3) and (6) into Eq. (1), the gas seepage governing equation in coal seams is obtained:

$$\nabla \left(-\frac{M p_g}{RT Z} \cdot \frac{k}{\mu} \nabla p_g \right) + \frac{\partial}{\partial t} \left(\frac{p_g ab}{1 + bp_g} \rho_c \cdot \frac{M p_g}{RT Z} + \varphi \cdot \frac{M p_g}{RT Z} \right) = 0 \quad (7)$$

It can be observed from Eq. (7) that porosity and permeability of coal seams are the key parameters in the gas extraction process, and the porosity is defined as (Li et al. 2016; Cui and Bustin 2005; Xia et al. 2015)

$$\varphi = \alpha - (\alpha - \varphi_0) \exp(S_0 - S), \quad (8)$$

where φ_0 is the initial porosity, α is the Biot coefficient and $\alpha = 1 - (K/K_s)$, K (GPa) is the bulk modulus of coal and $K = E/3(1 - 2\nu)$, K_s (GPa) is the bulk modulus of coal skeleton and $K_s = E_s/3(1 - 2\nu)$, ε_v is the volume strain of coal, S is the pore strain of coal and $S = \varepsilon_v + p_g/K - \varepsilon_a$, S_0 is the initial pore strain of coal and $S_0 = \varepsilon_{v0} + p_{g0}/K - \varepsilon_{a0}$. The subscript '0' represents the initial value of the corresponding variable. The relationship between permeability and porosity of coal seams can be described by the cubic law as follows

$$\frac{k}{k_0} = \left(\frac{\varphi}{\varphi_0} \right)^3, \quad (9)$$

where k_0 (m²) represents the initial permeability of coal seams. Substituting Eq. (8) into Eq. (9), the detailed permeability equation is obtained

$$k = k_0 \left[\frac{\alpha}{\varphi_0} - \left(\frac{\alpha}{\varphi_0} - 1 \right) \exp(S_0 - S) \right]^3 \quad (10)$$

Mechanical governing field

Based on the assumption, the total strain of coal is the result of stress, gas pressure and gas desorption, the relationship between stress and strain of coal can be expressed by (Wu et al. 2010)

$$\varepsilon_{ij} = \frac{1}{2G} \sigma_{ij} - \left(\frac{1}{6G} - \frac{1}{9K} \right) \sigma_{kk} \delta_{ij} + \frac{\alpha p_g}{3K} \delta_{ij} + \frac{\varepsilon_a}{3} \delta_{ij}, \quad (11)$$

where G (GPa) represents the shear modulus of coal and $G = E/2(1 + \nu)$, E (GPa) and E_s (GPa) denotes the elastic modulus of coal and coal skeleton, ν denotes the Poisson's ratio, δ_{ij} denotes the Kronecker factor and ε_a denotes strain induced by skeleton gas adsorption. Furthermore, the geometric equation of coal deformation satisfies the Cauchy equation as follows

$$\varepsilon_{ij} = \frac{u_{i,j} + u_{j,i}}{2}, \quad (12)$$

where $u_{i,j}$ is the partial derivative in the j direction of the displacement in the i direction, $u_{j,i}$ is the partial derivative in the i direction of the displacement in the j direction. According to the elastic mechanics equation, the static equilibrium relationship of coal is expressed as

$$\sigma_{ij,j} + F_i = 0, \quad (13)$$

where F_i (MPa) is the volume force. Combining Eqs. (11), (12) and (13), the mechanical field governing equation of coal–gas coupling is obtained

$$Gu_{i,jj} + \frac{G}{1-2\nu}u_{j,ji} - \alpha p_{g,i} - K\varepsilon_{s,i} + F_i = 0 \tag{14}$$

The cross-coupling and the HM governing equations of gas extraction is illustrated in Fig. 2.

A multilateral-well case

Computational model

Based on the mathematical coupling model of coal deformation and gas flow proposed in this paper, an idealized of gas extraction model with multilateral wells is established, as shown in Fig. 3. The computational domain is

a 400 m × 400 m × 5 m hexahedral located at a depth of 800–805 m. There is a main wellbore with a radius of 0.15 m at the longitudinal center of coal seam and 4 lateral wells with a radius of 0.10 m at the horizontal center of coal seam. The length of lateral wells is 100 m, and the angle between two adjacent lateral well is 90°.

Initial and boundary conditions

The initial gas pressure of coal seams and the extraction pressure of boreholes are set as 0.7 MPa and 0.076 MPa, respectively. The upper boundary pressure of coal seams is equal to the overburden pressure of 20 MPa, and the bottom boundary is fixed. The surrounding boundary is bounded by the normal displacement and all external boundaries are insulated. The other major parameters are listed in Table. 1.

Fig. 2 Cross-coupling and the HM governing equations of gas extraction

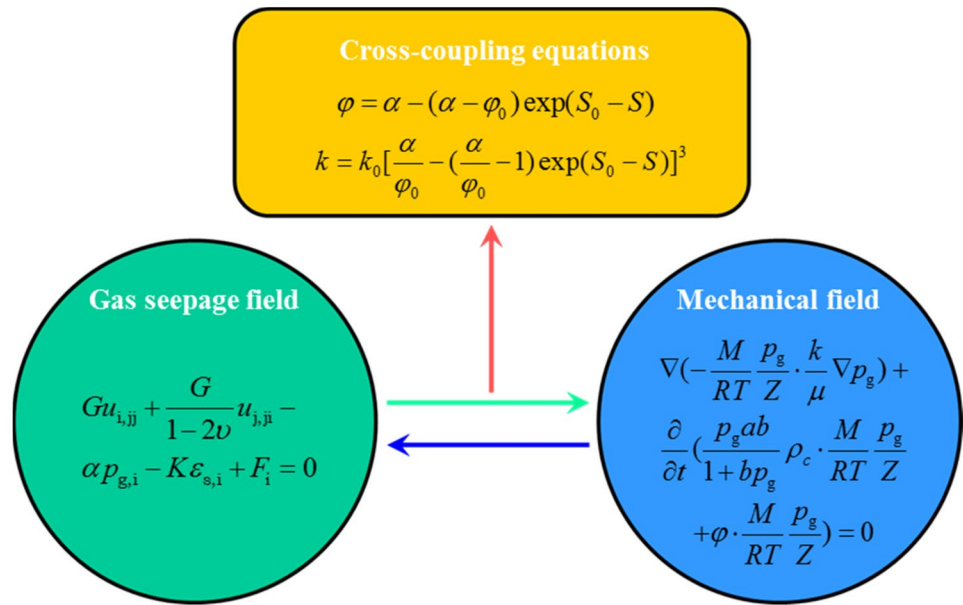


Fig. 3 Schematic of the computational model

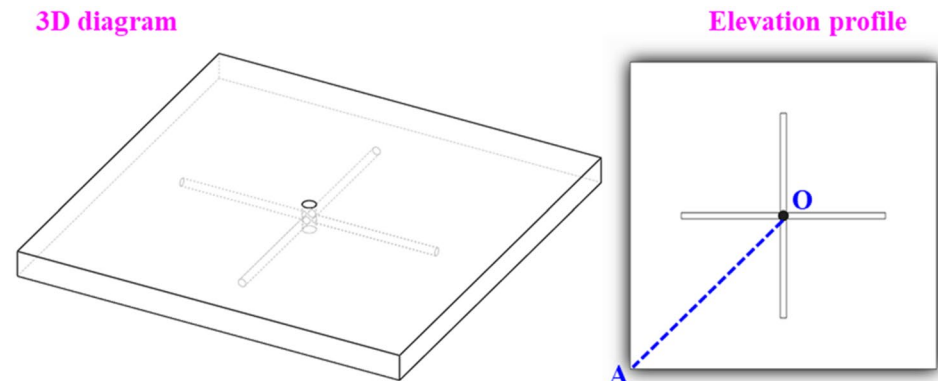


Table 1 Model basic parameters

Description	Value
Initial gas pressure of coal seam, MPa	0.7
Extraction pressure of boreholes, MPa	0.076
Initial permeability of coal seam, m ²	2.0 × 10 ⁻¹⁵
Elastic modulus of coal, GPa	2.713
Elastic modulus of coal skeleton, GPa	8.469
Poisson's ratio of coal, /	0.32
Initial porosity of coal, /	0.04
Dynamic viscosity of gas, Pa·s	1.03 × 10 ⁻⁵
Density of coal seams, kg/m ³	1380
Density at standard conditions of gas, kg/m ³	0.717
Langmuir adsorption constant, m ³ /kg	0.03832
Langmuir pressure constant, 1/Pa	5.11 × 10 ⁻⁷
Adsorption strain coefficient, kg/m ³	0.06
Temperature of coal seams, K	298.5

Description of well arrangements

Figure 4 illustrates sectional views of 12 different well arrangements. In Fig. 4, the white circular planes represent the main wellbore, the blue lines represent lateral wells, the red lines represent the drainage hole and the gray region represent coal seams.

For Case 2, Base Case and Case 5, the number of lateral wells is 2, 4, 6 and the total length of lateral wells is 200 m, 400 m and 600 m, respectively. For Case 1, Case 3 and Case 5, the number of drainage holes is 1, 2, 3 and the total length of drainage holes is 200 m, 400 m, 600 m, respectively. These six Cases are designed to compare the effect of gas extraction performance of coal seams with multilateral well and drainage holes.

For Case 6, the length of lateral wells is 95 m, 105 m, 95 m and 105 m from ① to ④, respectively. For Case 7, the length of lateral wells is 90 m, 110 m, 90 m and 110 m from ① to ④, respectively. For Case 8, the length of lateral wells is 95 m, 95 m, 105 m and 105 m from ① to ④, respectively. For Case 9, the length of lateral wells is 90 m, 90 m, 110 m and

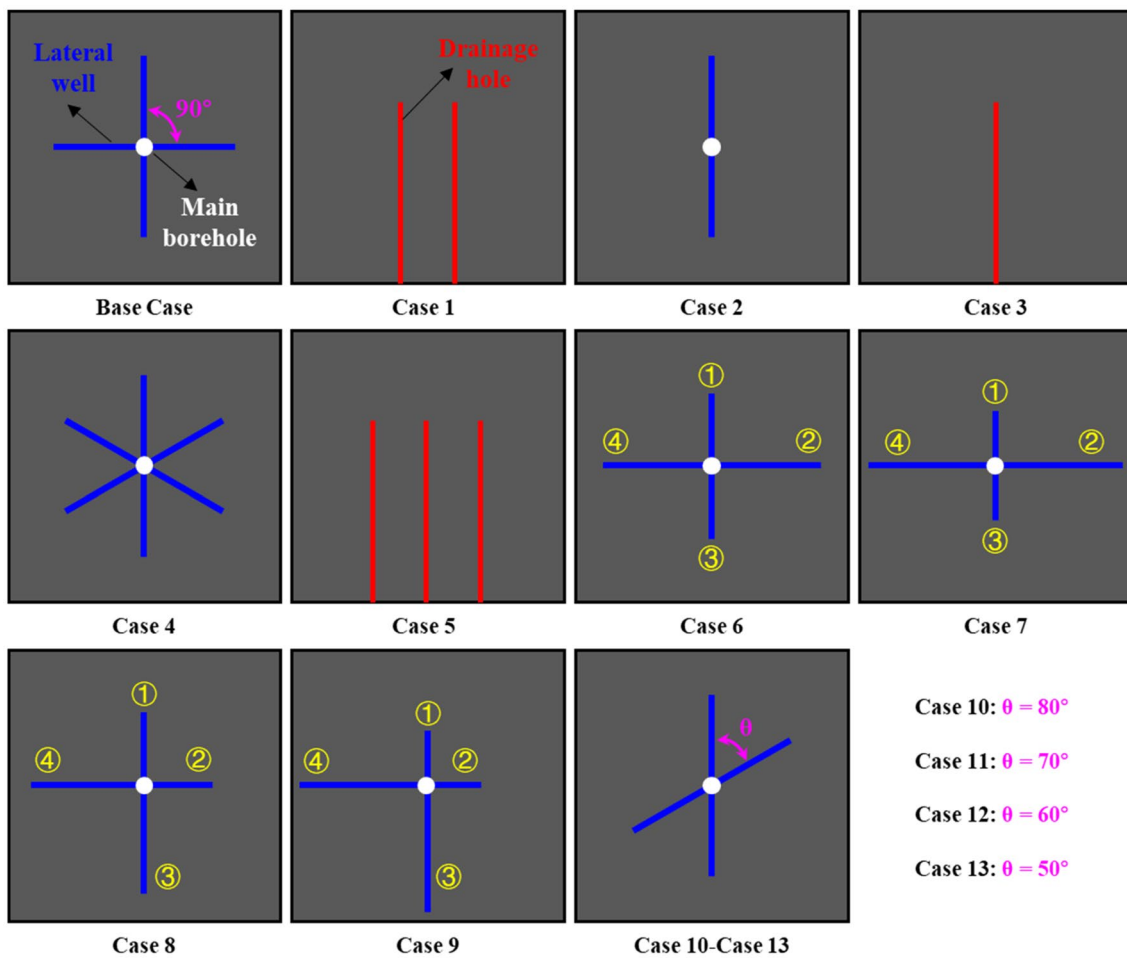


Fig. 4 Sectional views of 13 different well arrangements

110 m from ① to ④, respectively. The total length of lateral wells is equal of 400 m for Base Case and Case 6–9, these 5 Cases are designed to investigate the effect of lateral length distribution on gas extraction performance.

For Base Case, the angle between two adjacent lateral wells is 90° . In order to study the effect of angle between lateral well on gas extraction performance, Case 10–Case 13 are designed. From Case 10 to Case 13, the minimum angle between two adjacent lateral wells is 80° , 70° , 60° and 50° , respectively.

Results and discussion

Analysis of pressure and permeability rate variation

In order to study the gas extraction process in coal seams, variation of pressure distribution and permeability rate distribution was analyzed. The pressure contours and permeability ratio under different times of 10 d, 50 d, 100 d, 200 d, 600 d, 1200 d, 2000 d and 3000 d were investigated as shown in Figs. 5 and 6, respectively. As Fig. 5 demonstrates that the pore pressure decreases and its variation rate decreases

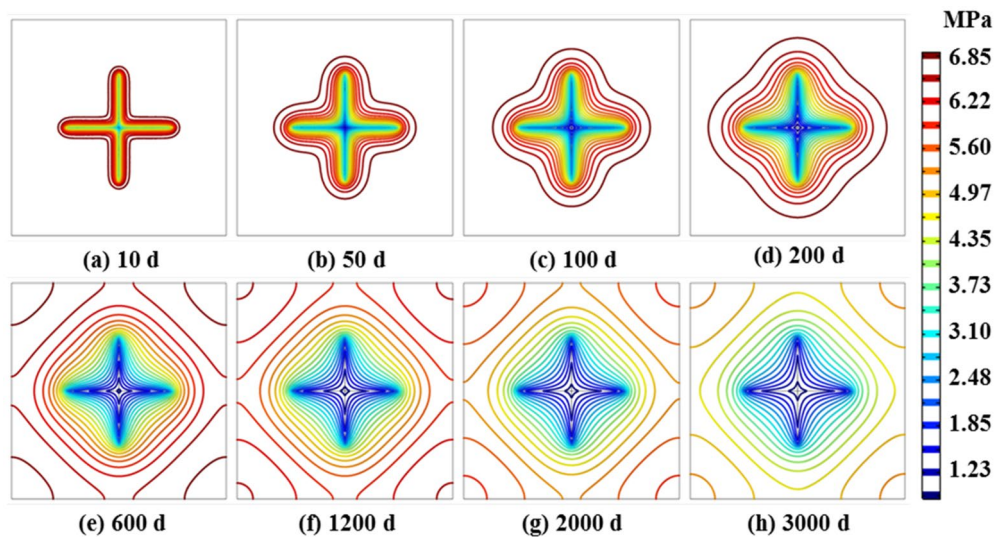


Fig. 5 Pressure contours distribution at different times

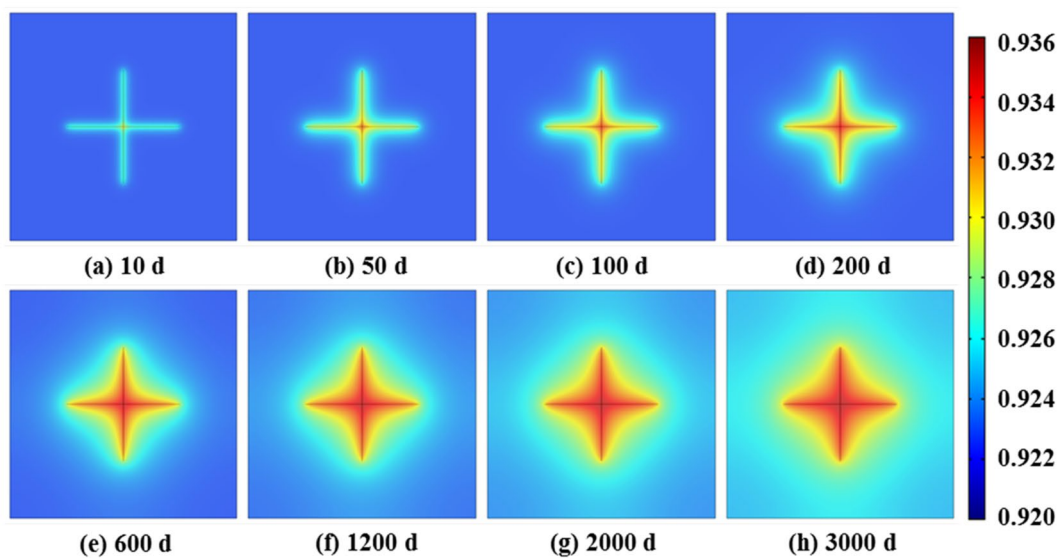


Fig. 6 Permeability ratio distribution at different times

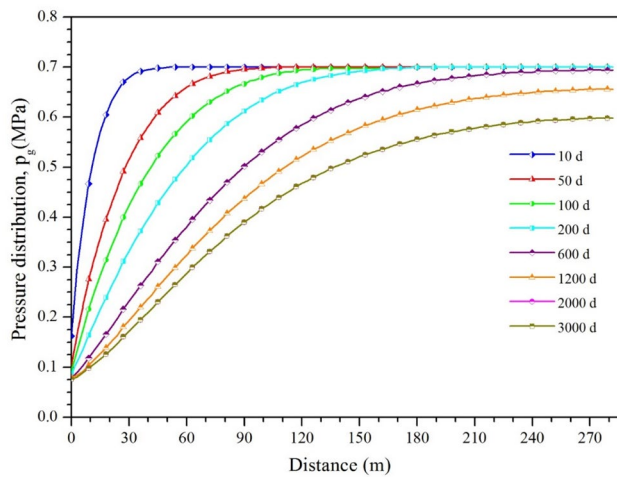


Fig. 7 Pressure distribution variation curve versus distance along line OA at various times

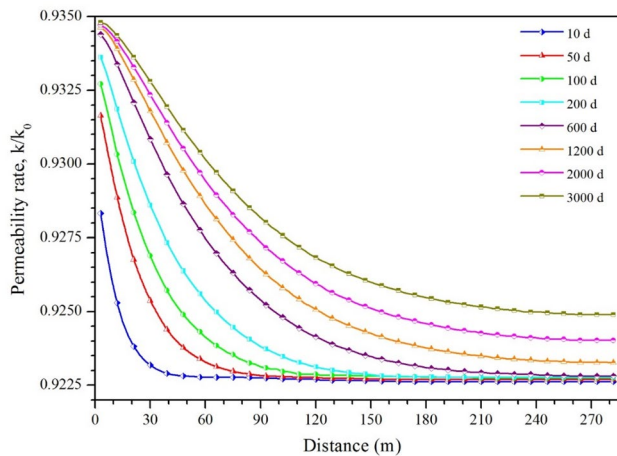


Fig. 8 Permeability ratio variation curve versus distance along line OA at various times

gradually with production time. There is a minimum gas pressure distribution around the multilateral well, and the pressure around the multilateral well decreases faster than the area away from the multilateral well. It can be observed from Fig. 6 that the overall permeability of coal seams increases with production time. The permeability around the multilateral well is larger than the area away from the multilateral well. This is because the gas pressure around the multilateral-well drops rapidly which leads to the gas first desorbs from the matrix around the multilateral well, causing the matrix in the corresponding area begin to shrink and the permeability gradually increases.

The pressure distribution and permeability ratio distribution along Line OA at various times are demonstrated in Figs. 7, 8, respectively. Line OA is marked in the second

picture in Fig. 3, and it is along the diagonal direction along the xy plane at mid- y position. It can be observed that the permeability ratio decreases with distance from reservoir center and its variation distance decreases with the extraction time. When the distance increases from 10 to 270 m, the permeability rate decreases from 0.9253 to 0.9226 at the 10 d, decreases from 0.9334 to 0.9228 at the 600 d and decreases from 0.9344 to 0.9249 at the 3000 d. At the same distance, the permeability ratio increases with the extraction time. When the extraction time ranges from 10 to 3000 d, the permeability ratio increases from 0.9228 to 0.9309 in the 50 m position, increases from 0.9227 to 0.9277 in the 100 m position and increases from 0.9226 to 0.9252 in the 200 m position.

Comparisons of multilateral-well case and drainage hole case

In this part, the coalbed methane development performance of multilateral-well Case and drainage holes Case were compared. There are three multilateral-well Cases and three drainage hole Cases for comparison. The specific results are as follows.

Comparisons of base case and case 1

In this section, effects of the four lateral wells (Base Case) and double drainage holes (Case 1) on coalbed methane development performance are studied. The pressure and permeability rate contours of gas extraction for Base Case and Case 1 at 50 d, 500 d, 1500 d and 3000 d are illustrated in Figs. 9, 10, respectively. It can be observed that the low-pressure and high-permeability region expands with time. The low-pressure and high-permeability spreads from the reservoir center to the surroundings for Base Case and from the bottom of the reservoir for Case 1. The location of the spread center depends on the location of the production well. For Base Case, the pressure difference between high pressure and low pressure is less than that of Case 1 at 3000 d. The permeability ratio difference also has the same effect. It can be concluded that the gas extraction area of the multilateral well is wider and more uniform than that of drainage hole Case.

To figure out the gas extraction performance of multilateral well and drainage hole, the production rate and cumulative production of Base Case and Case 1 are compared, as shown in Fig. 11. Under the condition that only single-phase flow is considered, the production rate shows a downward trend, the initial production rate drops rapidly and the speed in the middle and late stages of production tends to be stable. For instance, the production rate of Base Case varies from 991.32 m^3/d (100 d), 388.52 m^3/d (1000 d), 293.35 m^3/d (2000 d) to 241.99 m^3/d (3000 d). The production rate of the

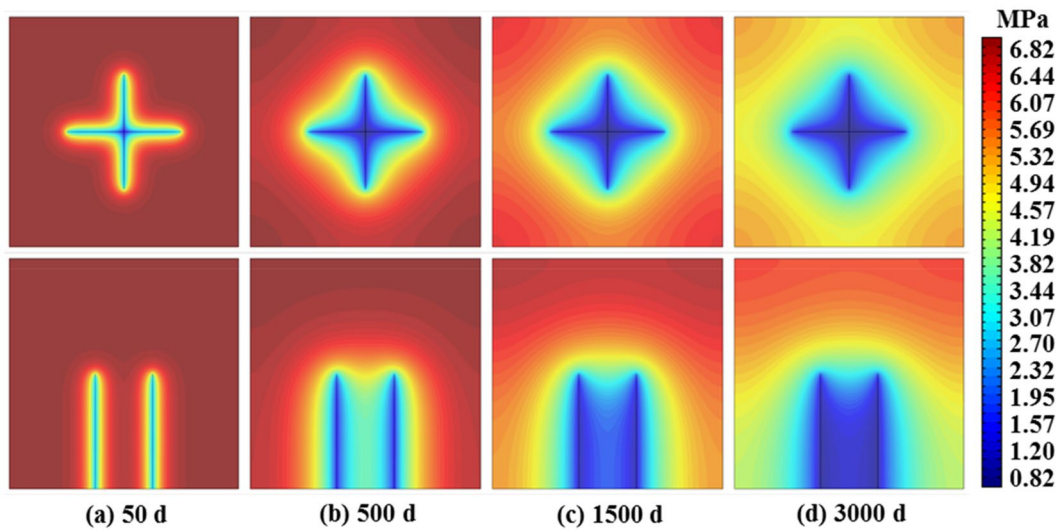


Fig. 9 Pressure contours of gas extraction at 50 d, 500 d, 1500 d and 3000 d (first row: Base Case, second row: Case 1)

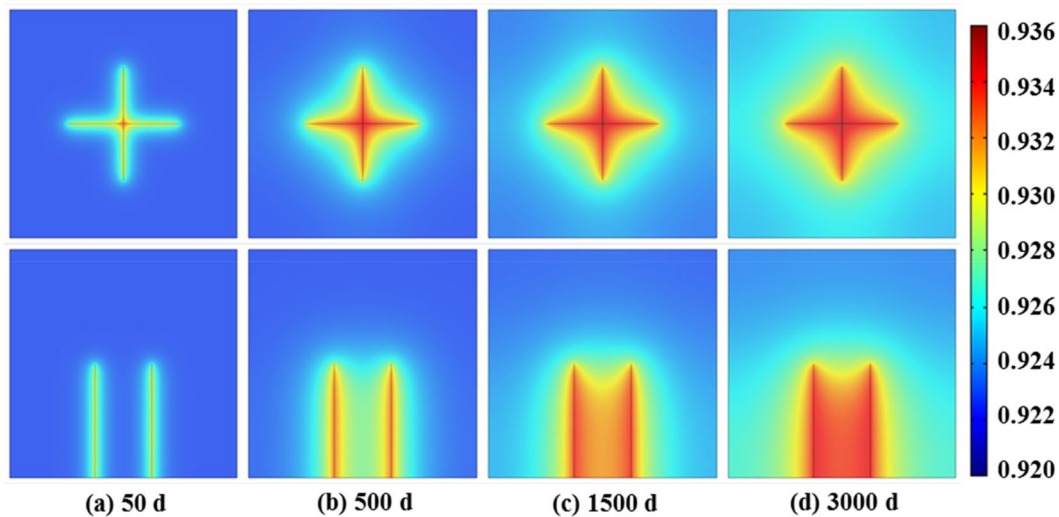


Fig. 10 Permeability ratio (k/k_0) contours of gas extraction at 50 d, 500 d, 1500 d and 3000 d (first row: Base Case, second row: Case 1)

Base Case is always higher than that of Case 1. Similarly, the cumulative production of the Base Case is always higher than that of Case 1 and the ultimate cumulative production of Base Case is almost 1.27 times higher than that of Case 1.

Comparisons of case 2 and case 3

In this section, effects of the double lateral wells (Case 2) and single drainage hole (Case 3) on coalbed methane development performance are studied. The pressure and permeability ratio contours of gas extraction for Case 2 and Case 3 at 50 d, 500 d, 1500 d and 3000 d are illustrated in Fig. 12, 13, respectively. It can be seen that the similar pressure and

permeability ratio distribution effect as that of Base Case and Case 2. The low-pressure and high-permeability spreads from the reservoir center to the surroundings for Case 2 and from the bottom of the reservoir for Case 3.

Figure 14 shows the production rate and cumulative production of Case 2 and Case 3. The production rate of Case 2 varies from 579.59 m³/d (100 d) to 205.51 m³/d (3000 d), and Case 3 varies from 463.55 m³/d (100 d) to 145.91 m³/d (3000 d). The production rate of the Case 2 is always higher than that of Case 3. The cumulative production of Case 2 varies from 0.6261×10^5 m³ (100 d) to 8.6416×10^5 m³ (3000 d), and Case 3 varies from 0.5022×10^5 m³ (100 d) to 6.4341×10^5 m³ (3000 d). The ultimate cumulative

Fig. 11 Production rate and cumulative production curve versus time for Base Case and Case 1

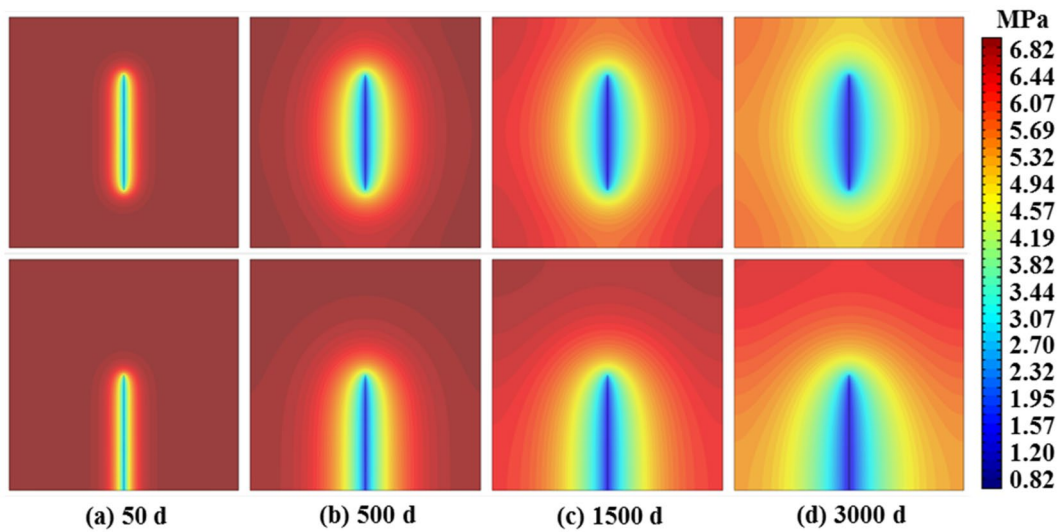
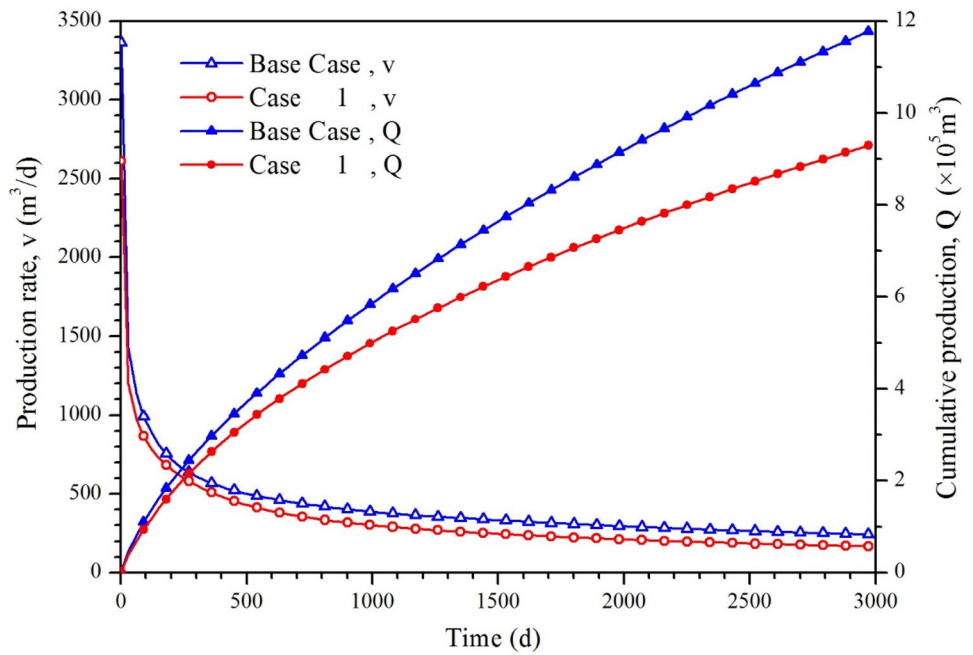


Fig. 12 Pressure contours of gas extraction at 50 d, 500 d, 1500 d and 3000 d (first row: Case 2, second row: Case 3)

production of Case 2 is almost 1.34 times higher than that of Case 3 at 3000 d.

Comparisons of case 4 and case 5

In this section, effects of the six lateral wells (Case 4) and three drainage holes (Case 5) on coalbed methane development performance are studied. The pressure and permeability ratio contours of gas extraction for Case 4 and Case 5 at 50 d, 500 d, 1500 d and 3000 d are illustrated in Figs. 12, 13, respectively. It can be seen that the similar pressure and

permeability distribution effect as that of Base Case and Case 2 (Figs. 15, 16). The low-pressure and high-permeability spreads from the reservoir center to the surroundings for Case 4 and from the bottom of the reservoir for Case 5.

Figure 17 shows the production rate and cumulative production of Case 4 and Case 5. The production rate of Case 4 varies from 1200.6 m³/d (100 d) to 235.92 m³/d (3000 d), and Case 5 varies from 1277.1 m³/d (100 d) to 174.2 m³/d (3000 d). In the first 900 d, the production rate of Case 5 is higher than that of Case 4, while the production rate of Case 4 is higher than that of Case 5 after 900 d. The

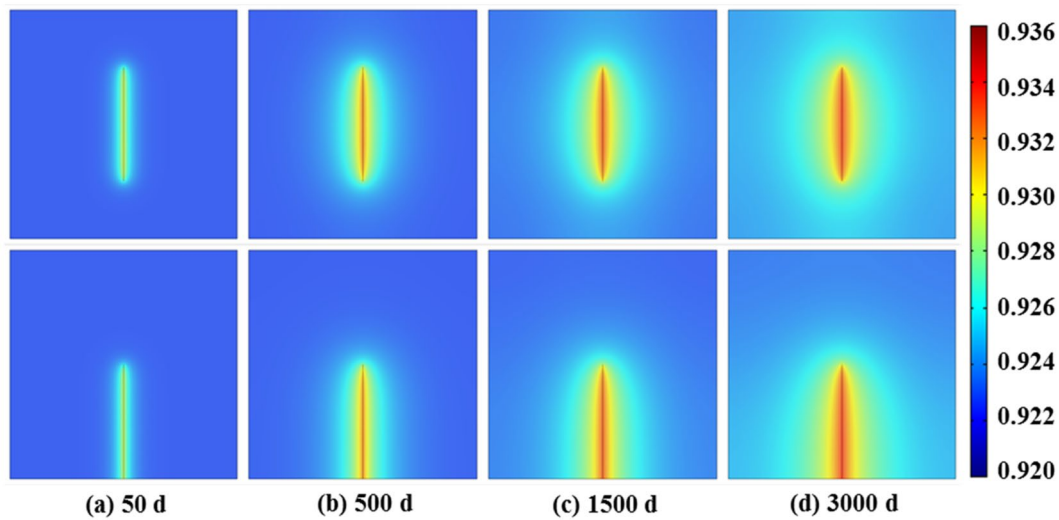
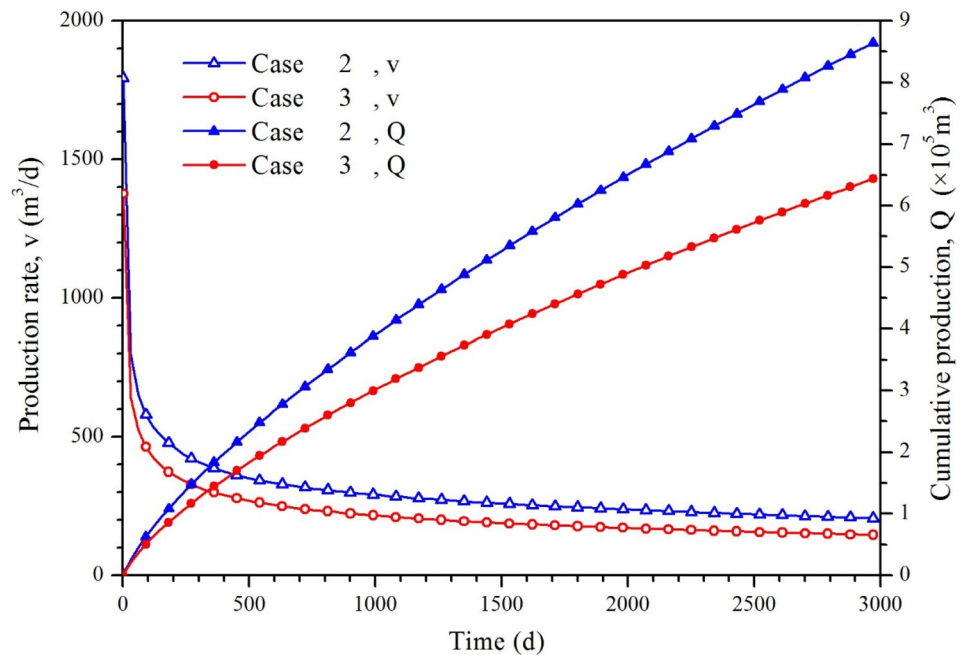


Fig. 13 Permeability ratio contours of gas extraction at 50 d, 500 d, 1500 d and 3000 d (first row: Case 2, second row: Case 3)

Fig. 14 Production ratio and cumulative production curve versus time for Case 2 and Case 3



cumulative production of Case 4 varies from 1.4064×10^5 m³ (100 d) to 12.4845×10^5 m³ (3000 d) and Case 5 varies from 1.3834×10^5 m³ (100 d) to 1.2179×10^6 m³ (3000 d). The ultimate cumulative production of Case 4 is almost 1.025 times higher than that of Case 5 at 3000 d.

The cumulative production statistics for Base Case and Case1–Case 5 are illustrated in Fig. 18. A comparison of the results reveals the coalbed methane development performance of multilateral-well Case is better than that of drainage holes Case. The ultimate cumulative production of four lateral wells is almost 1.27 times than that of drainage holes.

When the quantity of lateral wells increases from 2 to 6, the cumulative production at 3000 d increases by a factor of 1.5. There are two possible reasons. One is because the multilateral well located in the center of the reservoir are more stretched and have a larger area of influence. The second is that the radius of the multilateral well is larger than of the drainage hole and more gas flows into the multi-branched well.

For multilateral well, the cumulative production increases with the quantity of lateral wells. When the lateral well number is 2, 4, 6, the cumulative production

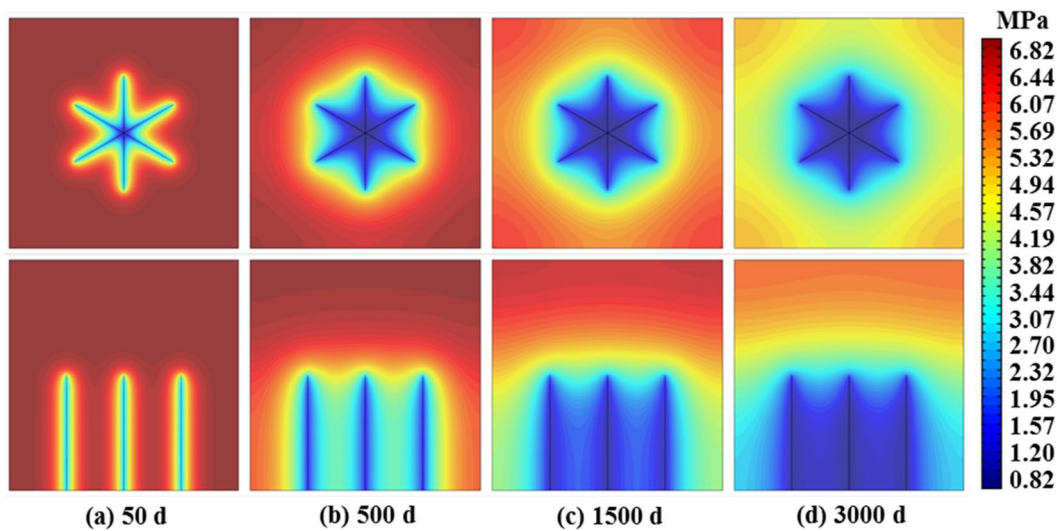


Fig. 15 Pressure contours of gas extraction at 50 d, 500 d, 1500 d and 3000 d (first row: Case 4, second row: Case 5)

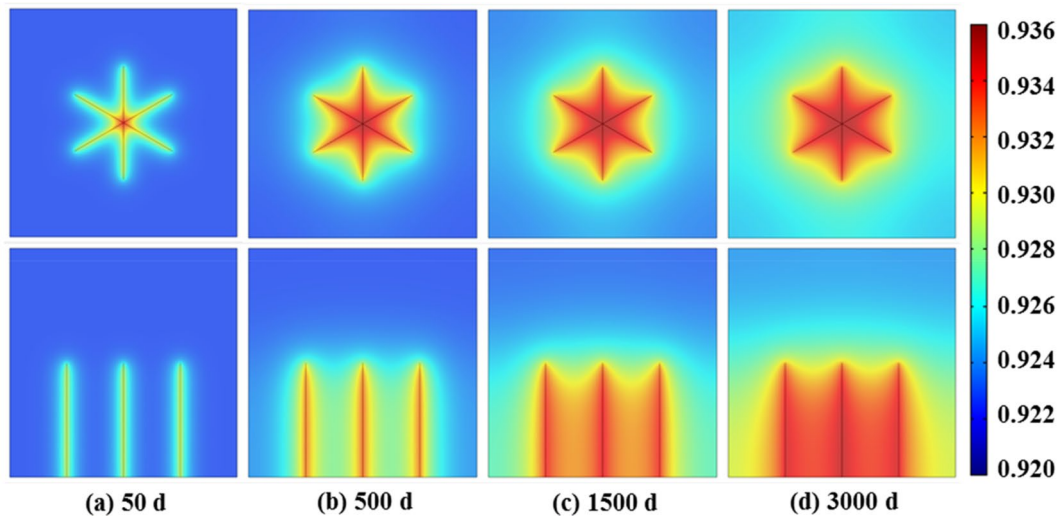


Fig. 16 Permeability ratio contours of gas extraction at 50 d, 500 d, 1500 d and 3000 d (first row: Case 4, second row: Case 5)

is $8.6416 \times 10^5 \text{ m}^3$, $11.7785 \times 10^5 \text{ m}^3$, $1.2445 \times 10^6 \text{ m}^3$ at 3000 d, respectively. The cumulative production increases obvious when the lateral well number vary from 2 to 4. It can be speculated that the coalbed methane development performance can be improved to a certain extent by increasing the quantity of lateral well.

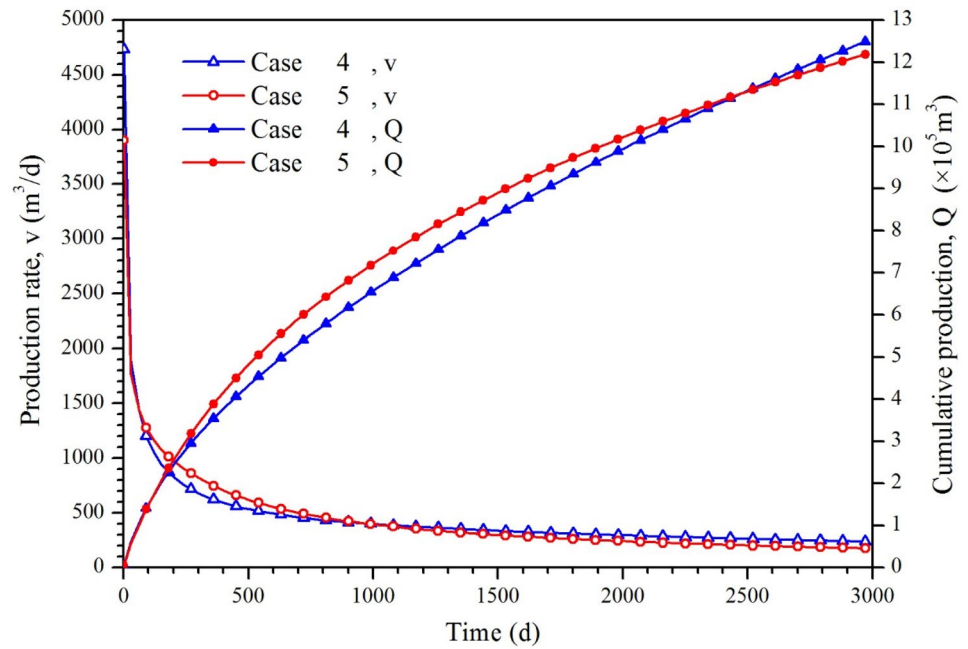
Comparisons of multilateral well with different branch length

In this section, the length distribution of lateral wells on coalbed methane development performance are studied. Figures 19, 20 show the pressure contours and permeability ratio contours of gas extraction at 50 d, 500 d, 1500 d and

3000 d for Case 6 and Case 7, respectively. The lateral wells of Case 6 and Case 7 are all axisymmetric, and the pressure and permeability at various times also show an axisymmetric distribution. Figures 21, 22 show the pressure contours and permeability ratio contours of gas extraction at 50 d, 500 d, 1500 d and 3000 d for Case 8 and Case 9, respectively. The lateral wells of Case 8 and Case 9 are all diagonally symmetric and their pressure and permeability at various times also symmetrically distributed diagonally. It suggests that the length distribution of lateral wells has an effect on regional gas extraction efficiency.

In order to figure out the gas extraction performance of multilateral well with different lateral length distribution, the production rate and cumulative production of Base

Fig. 17 Production rate and cumulative production curve versus time for Case 4 and Case 5



Case and Case 6–9 are compared, as shown in Fig. 23. It can be observed that when all the length of lateral wells is 100 m, the gas production rate and cumulative production are always higher than other Cases. When the lengths of the lateral wells are not equal, the ultimate gas production from high to low is Case 6, Case 8, Case 7 and Case 9, respectively.

For Case 6 and Case 8, there are two lateral wells of length 95 m and 105 m with a maximum length difference of 10 m. For Case 7 and Case 9, there are two lateral wells of length 90 m and 110 m with a maximum length difference of 20 m. The gas extraction performance of Case 6 and Case 8 are better than that of Case 7 and Case 9, it can be seen

that the uniform of length distribution has a positive effect on coalbed methane development. The difference between the Case6 and Case 8 is that the lateral length distribution is different. The lateral wells of Case 6 are center-symmetrical, long lateral well and short lateral well are alternately distributed, it can produce CBM in the gas reservoir more uniformly. Therefore, the gas extraction performance of Case 6 is higher than that of Case 8. The gas extraction performance of Case 7 and Case 9 can also explain by the symmetry of length distribution.

Overall, when the total length of lateral wells is equal, the uniformity and symmetry of lateral length distribution are two key factors on the gas extraction performance. Under the simulation condition in this paper, the uniformity of lateral length distribution has a greater impact on the gas extraction performance than that of symmetry.

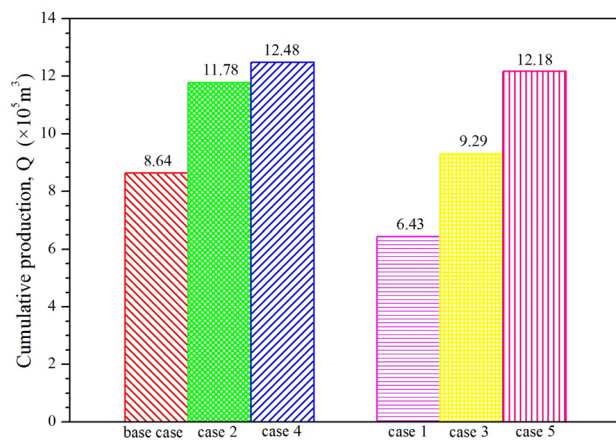


Fig. 18 Cumulative production statistics for Base Case and Case 1–Case 5

Comparisons of multilateral well with different intersection angle

In this section, the intersection angle of lateral wells on coalbed methane development performance are studied. Figures 24, 25 show the pressure contours of gas extraction at 50 d, 500 d, 1500 d and 3000 d for Case 10–11 and Case 12–13, respectively. Figures 26, 27 show the permeability ratio contours of gas extraction at 50 d, 500 d, 1500 d and 3000 d for Case 10–11 and Case 12–13, respectively. It can be observed that the pressure and permeability distribution difference induced by different intersection angle of lateral wells.

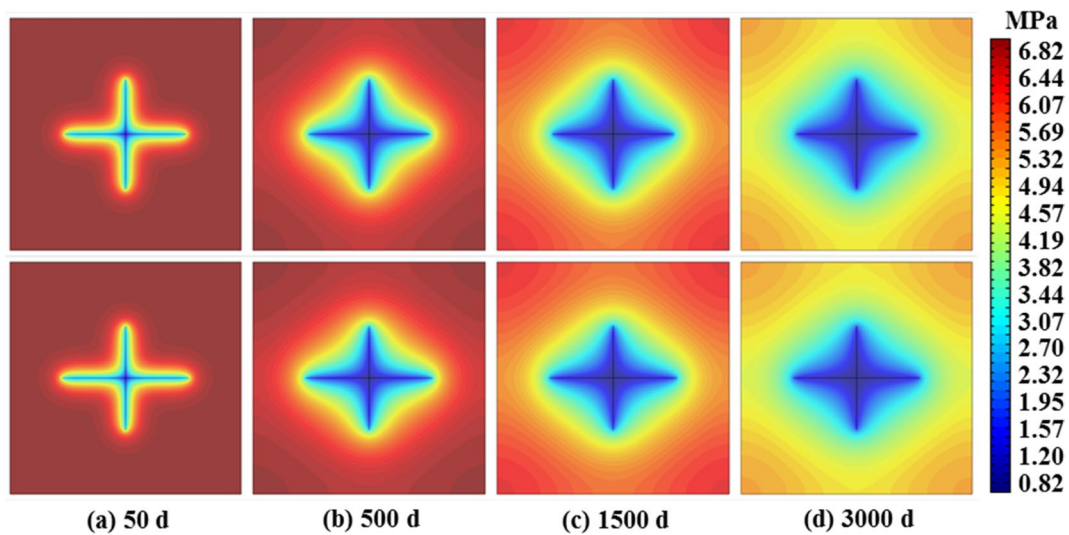


Fig. 19 Pressure contours of gas extraction at 50 d, 500 d, 1500 d and 3000 d (first row: Case 6, second row: Case 7)

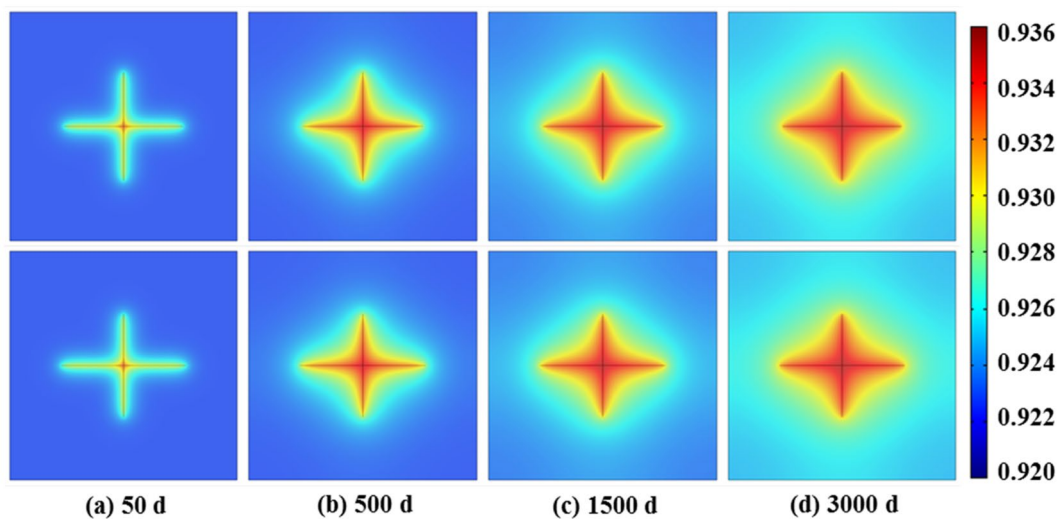


Fig. 20 Permeability ratio contours of gas extraction at 50 d, 500 d, 1500 d and 3000 d (first row: Case 6, second row: Case 7)

Figure 26 shows the production rate and cumulative production of Base Case and Case 10–13. When the intersection angle varies from 90° to 50°, the ultimate cumulative production decrease from $1.1779 \times 10^6 \text{ m}^3$ (90°), $1.1464 \times 10^6 \text{ m}^3$ (80°), $1.1360 \times 10^6 \text{ m}^3$ (70°), $1.1259 \times 10^5 \text{ m}^3$ (60°) to $1.1086 \times 10^6 \text{ m}^3$ (50°) at 3000 d. It can be observed that the minimum intersection angle has a positive effect on cumulative production as shown in Fig. 28. This is because when the intersection angle varies from 90° to 50°, the quadrilateral area with the lateral well as

the diagonal decreases gradually. The smaller the quadrilateral area, the smaller the influence range of the multilateral well and the worse the gas extraction effect. When the intersection angle of the multilateral well is set as 90°, the wells are more stretched and the quadrilateral area is larger than other Cases. Overall, the optimal intersection angle is 90° for the multilateral well under the simulation condition in this paper.

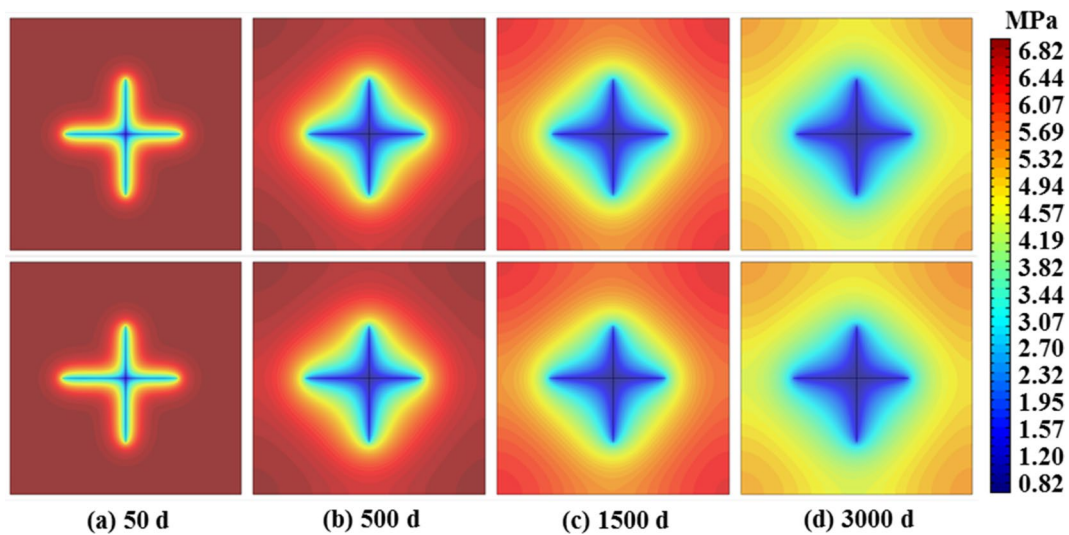


Fig. 21 Pressure contours of gas extraction at 50 d, 500 d, 1500 d and 3000 d (first row: Case 8, second row: Case 9)

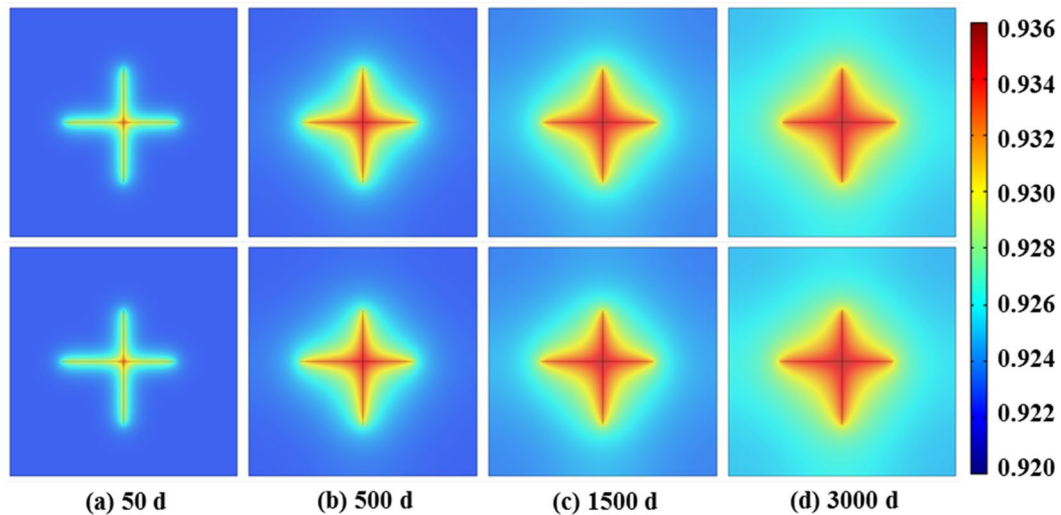


Fig. 22 Permeability ratio contours of gas extraction at 50 d, 500 d, 1500 d and 3000 d (first row: Case 8, second row: Case 9)

Conclusion

In this paper, a novel multilateral well for coalbed methane extraction was proposed. In the multilateral-well system, there is a main wellbore at the longitudinal center of coal seam and four lateral wells at the horizontal center. The coalbed methane development performance of multilateral-well Case is better than that of traditional drainage holes. A hydraulic-mechanical coupling model was established for the novel multilateral-well system. Based

on the model, the pressure distribution and permeability distribution of the gas extraction process with multilateral well were analyzed comprehensively. Subsequently, the gas extraction performance with multilateral well and drainage holes were compared. The number, length distribution and intersection angle of multilateral-well system on the gas extraction performance were investigated. The key findings of the study were as follows.

Fig. 23 Production rate and cumulative production curve versus time for Base Case, Case 6, Case 7, Case 8 and Case 9

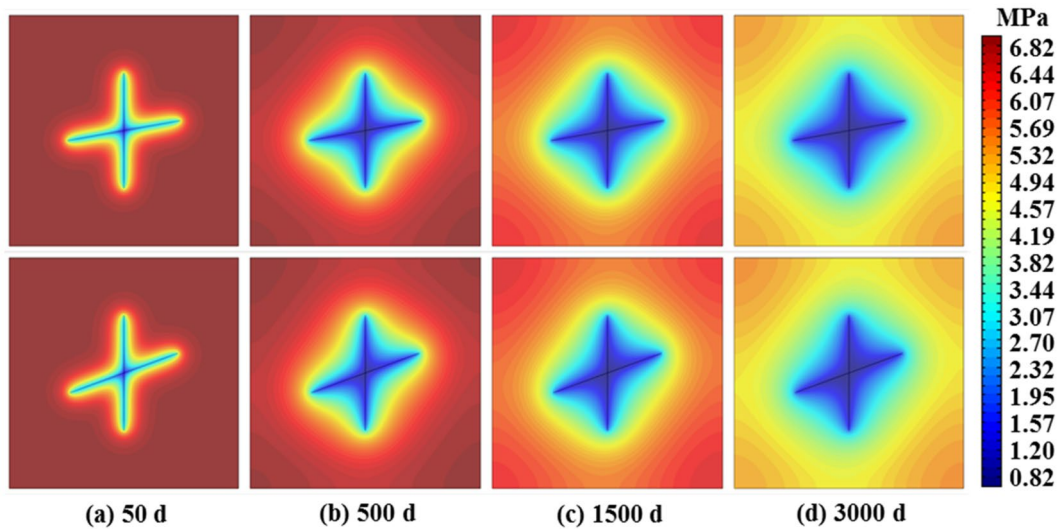
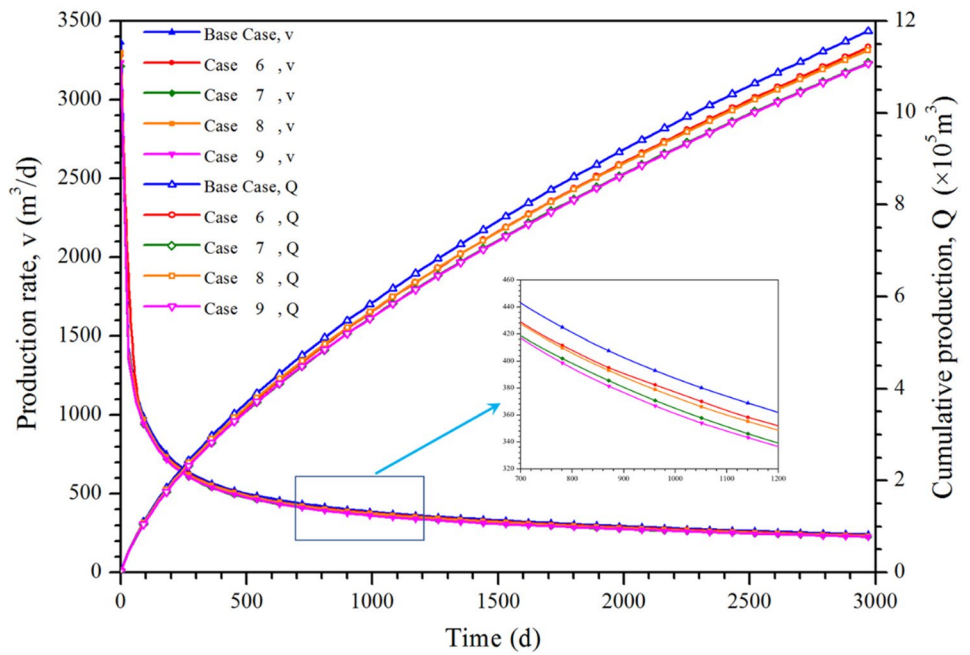


Fig. 24 Pressure contours of gas extraction at 50 d, 500 d, 1500 d and 3000 d (first row: Base Case, second row: Case 10, third row: Case 11)

- (1) There is a minimum gas pressure distribution around the multilateral well and the pressure around the multilateral well decreases faster than the area away from the multilateral well. The overall permeability of coal seams increases with production time and the permeability around the multilateral well is larger than the area away from the multilateral well. This is because the gas pressure around the multilateral-well drops rapidly which leads to the gas first desorbs from the matrix around the multilateral well, causing the matrix in the corresponding area begin to shrink and the permeability gradually increases.
- (2) The coalbed methane development performance of multilateral-well Case is better than that of drainage

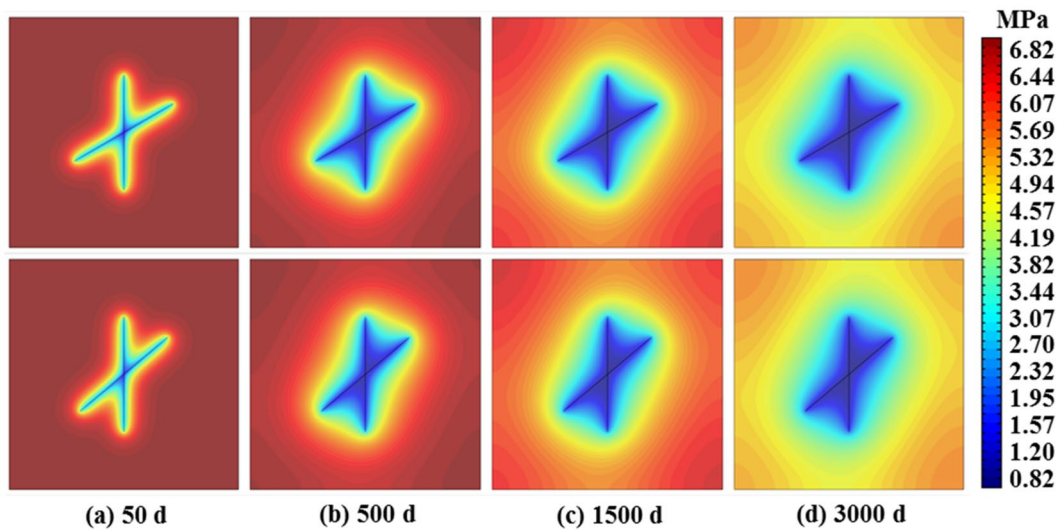


Fig. 25 Pressure contours of gas extraction at 50 d, 500 d, 1500 d and 3000 d (first row: Base Case, second row: Case 12, third row: Case 13)

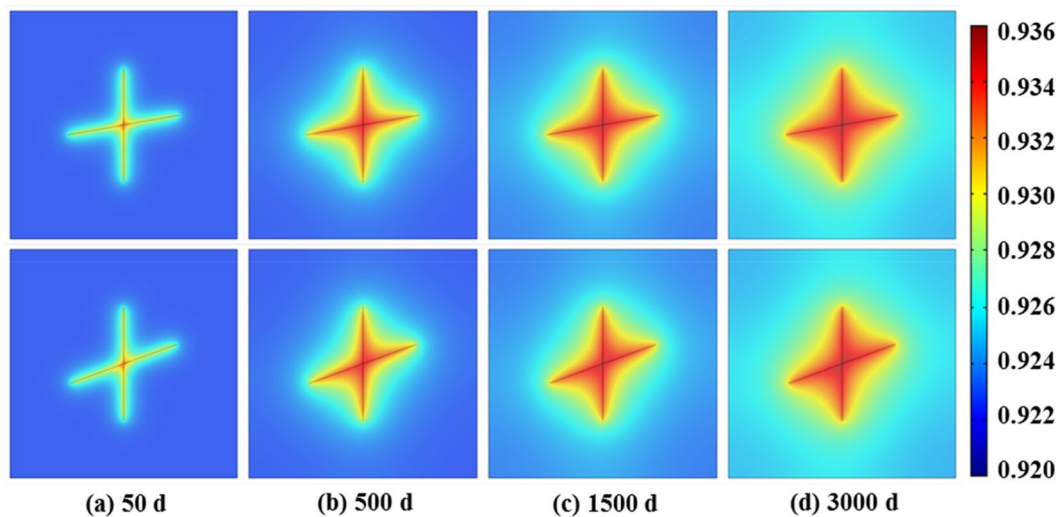


Fig. 26 Permeability ratio contours of gas extraction at 50 d, 500 d, 1500 d and 3000 d (first row: Case 10, second row: Case 11)

holes Case. The ultimate cumulative production of four lateral wells is almost 1.27 times than that of drainage holes. This is because the multilateral well located in the center of the reservoir are more stretched and have a larger area of influence. Besides, the radius of the multilateral well is larger than of the drainage hole and more gas flows into the multi-branched well.

- (3) The coalbed methane development performance can be improved to a certain extent by increasing the quantity of lateral well. When the quantity of lateral wells increases from 2 to 6, the cumulative production at 3000 d increases by a factor of 1.5.
- (4) When the total length of lateral wells is equal, the uniformity and symmetry of lateral length distribution are two key factors on the gas extraction performance.

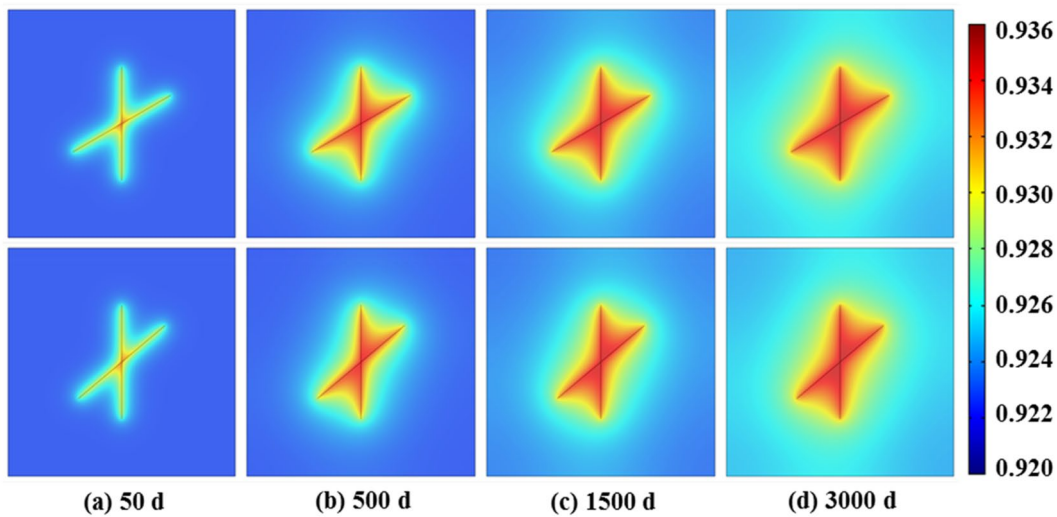
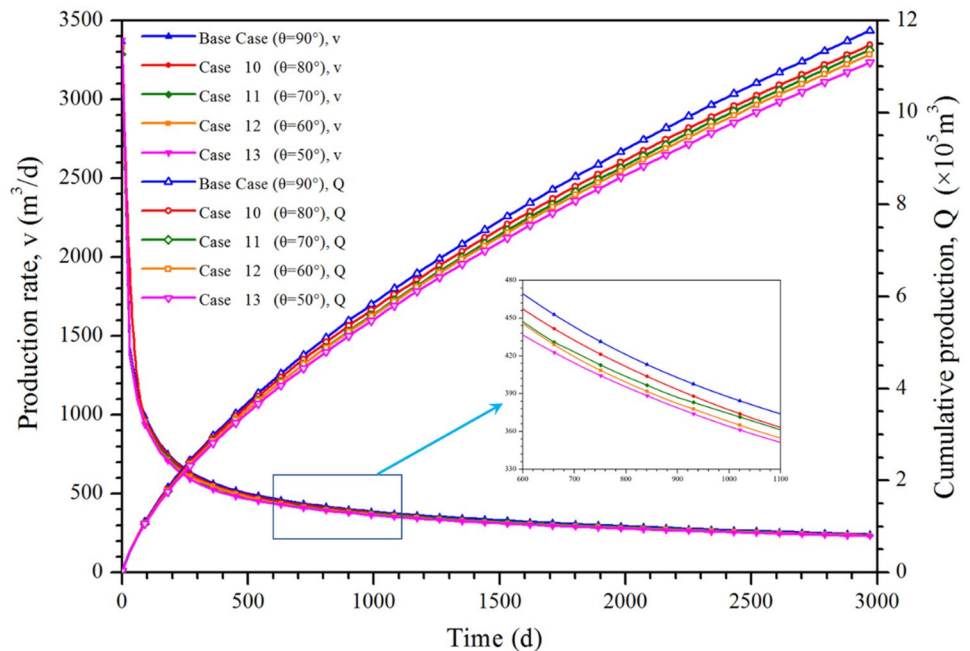


Fig. 27 Permeability ratio contours of gas extraction at 50 d, 500 d, 1500 d and 3000 d (first row: Case 12, second row: Case 13)

Fig. 28 Production rate and cumulative production curve versus time for Base Case, Case 10 and Case 11



Under the simulation condition in this paper, the uniformity of lateral length distribution has a greater impact on the gas extraction performance than that of symmetry.

- (5) The minimum intersection angle has a positive effect on cumulative production. When the intersection angle varies from 90° to 50°, the cumulative production varies from $1.1779 \times 10^6 \text{ m}^3$ to $1.1086 \times 10^6 \text{ m}^3$. Under the simulation condition in this paper, the optimal intersection angle is 90° for the multilateral well.

Acknowledgements This work was supported by the National Natural Science Foundation of China (51474070). The authors would like to express sincere appreciation to the editor and the anonymous reviewers for their helpful comments on the paper.

Funding This work was supported by the National Natural Science Foundation of China (51474070).

Open Access This article is licensed under a Creative Commons Attribution 4.0 International License, which permits use, sharing, adaptation, distribution and reproduction in any medium or format, as long as you give appropriate credit to the original author(s) and the source, provide a link to the Creative Commons licence, and indicate if changes

were made. The images or other third party material in this article are included in the article's Creative Commons licence, unless indicated otherwise in a credit line to the material. If material is not included in the article's Creative Commons licence and your intended use is not permitted by statutory regulation or exceeds the permitted use, you will need to obtain permission directly from the copyright holder. To view a copy of this licence, visit <http://creativecommons.org/licenses/by/4.0/>.

References

- An H, Wei XR, Wang GX, Massarotto P, Wang FY, Rudolph V, Golding SD (2015) Modeling anisotropic permeability of coal and its effects on CO₂ sequestration and enhanced coalbed methane recovery. *Int J Coal Geol* 152:15–24. <https://doi.org/10.1016/j.coal.2015.09.013>
- Chen XX, Wang L, Xue L (2019a) A gaseous compound of hydrogen and carbon production performance model in coalbed reservoir with horizontal fractures. *Int J Hydrogen Energ* 44(11):5262–5269. <https://doi.org/10.1016/j.ijhydene.2018.08.081>
- Chen ZM, Liao XW, Zhao XL (2019b) A practical methodology for production-data analysis of single-phase unconventional wells with complex fracture geometry. *SPE Reserv Eval Eng* 22(02):458–476. <https://doi.org/10.2118/191372-PA>
- Cui X, Bustin RM (2005) Volumetric strain associated with methane desorption and its impact on coalbed gas production from deep coal seams. *Aapg Bull* 89(9):1181–1202. <https://doi.org/10.1306/05110504114>
- Fan L, Liu SM (2018) Numerical prediction of in situ horizontal stress evolution in coalbed methane reservoirs by considering both poroelastic and sorption induced strain effects. *Int J Rock Mech Min* 104:156–164. <https://doi.org/10.1016/j.ijrmm.2018.02.012>
- Fan CJ, Elsworth D, Li S, Zhou LJ, Yang ZH, Song Y (2019) Thermo-hydro-mechanical-chemical couplings controlling CH₄ production and CO₂ sequestration in enhanced coalbed methane recovery. *Energy* 173:1054–1077. <https://doi.org/10.1016/j.energy.2019.02.126>
- Feng RM, Liu J, Chen SN, Bryant S (2018) Effect of gas compressibility on permeability measurement in coalbed methane formations: experimental investigation and flow modeling. *Int J Coal Geol* 198:144–155. <https://doi.org/10.1016/j.coal.2018.09.010>
- Li T, Wu CF, Liu Q (2015) Characteristics of coal fractures and the influence of coal facies on coalbed methane productivity in the South Yanchuan Block, China. *J Nat Gas Sci Eng* 22:625–632. <https://doi.org/10.1016/j.jngse.2015.01.014>
- Li S, Fan CJ, Han J, Luo MK, Yang ZH, Bi HJ (2016) A fully coupled thermal-hydraulic-mechanical model with two-phase flow for coalbed methane extraction. *J Nat Gas Sci Eng* 33:324–336. <https://doi.org/10.1016/j.jngse.2016.05.032>
- Li MH, Liu GF, Liu XR, Li ZJ, Zhang Q, Shen BX (2019) Performance of a direct-injection natural gas engine with multiple injection strategies. *Energy* 2019:116363. <https://doi.org/10.1016/j.energy.2019.116363>
- Liu HH, Sang SX, Formolo M, Li MX, Liu SQ, Xu HJ, An SK, Li JJ, Wang XZ (2013) Production characteristics and drainage optimization of coalbed methane wells: a case study from low-permeability anthracite hosted reservoirs in southern Qinshui Basin China. *Energy Sustain Dev* 17(5):412–423. <https://doi.org/10.1016/j.esd.2013.04.005>
- Liu ZD, Cheng YP, Liu QQ, Jiang JY, Li W, Zhang KZ (2017a) Numerical assessment of CMM drainage in the remote unloaded coal body: insights of geostress-relief gas migration and coal permeability. *J Nat Gas Sci Eng* 45:487–501. <https://doi.org/10.1016/j.jngse.2017.06.017>
- Liu T, Lin BQ, Yang W, Liu T, Kong J, Huang ZB, Wang R, Zhao Y (2017b) Dynamic diffusion-based multifield coupling model for gas drainage. *J Nat Gas Sci Eng* 44:233–249. <https://doi.org/10.1016/j.jngse.2017.04.026>
- Liu T, Lin BQ, Yang W, Zhai C, Liu T (2017c) Coal permeability evolution and gas migration under non-equilibrium state. *Transport Porous Med* 118(3):393–416. <https://doi.org/10.1007/s11242-017-0862-8>
- Liu HH, Sang SX, Xue JH, Lan TH, Xu HJ, Ren B, Liu SQ (2018) Evolution and geochemical characteristics of gas phase fluid and its response to inter-well interference during multi-well drainage of coalbed methane. *J Petrol Sci Eng* 162:491–501. <https://doi.org/10.1016/j.petrol.2017.10.007>
- Luo DK, Dai YJ, Xia LY (2011) Economic evaluation based policy analysis for coalbed methane industry in China. *Energy* 36(1):360–368. <https://doi.org/10.1016/j.energy.2010.10.031>
- Luo CJ, Zhang DF, Lun ZM, Zhao CP, Wang HT, Pan ZJ, Li YH, Zhang J, Jia SQ (2019) Displacement behaviors of adsorbed coalbed methane on coals by injection of SO₂/CO₂ binary mixture. *Fuel* 247:356–367. <https://doi.org/10.1016/j.fuel.2019.03.057>
- Ma YY, Li SB, Zhang LG, Liu SZ, Liu ZY, Li H, Shi EX, Zhang HJ (2020a) Numerical simulation study on the heat extraction performance of multi-well injection enhanced geothermal system. *Renew Energ* 151:782–792. <https://doi.org/10.1016/j.renene.2019.11.067>
- Ma YY, Li SB, Zhang LG, Liu SZ, Liu ZY, Li H, Shi EX (2020b) Study on the effect of well layout schemes and fracture parameters on the heat extraction performance of enhanced geothermal system in fractured reservoir. *Energy* 202:117811. <https://doi.org/10.1016/j.energy.2020.117811>
- Mohammed N, Abbas AJ, Enyi GC, Suleiman SM, Edem DE, Abba M (2020) Alternating N₂ gas injection as a potential technique for enhanced gas recovery and CO₂ storage in consolidated rocks: an experimental study. *J Petrol Explor Prod Technol* 10:3883–3903. <https://doi.org/10.1007/s13202-020-00935-z>
- Moore R, Palmer I, Higgs N (2015) Anisotropic model for permeability change in coalbed-methane wells. *SPE Reserv Eval Eng* 18(04):456–462. <https://doi.org/10.2118/169592-PA>
- Mu FY, Zhong WZ, Zhao XL, Che CB, Chen YP, Zhu J, Wang B (2015) Strategies for the development of CBM gas industry in China. *Nat Gas Ind B* 2(4):383–389. <https://doi.org/10.1016/j.ngib.2015.09.013>
- Prabu V, Mallick N (2015) Coalbed methane with CO₂ sequestration: an emerging clean coal technology in India. *Renew Sust Energ Rev* 50:229–244. <https://doi.org/10.1016/j.rser.2015.05.010>
- Qin Y, Moore TA, Shen J, Yang ZB, Shen YL, Wang J (2018) Resources and geology of coalbed methane in China: a review. *Int Geol Rev* 60(5–6):777–812. <https://doi.org/10.1080/00206814.2017.1408034>
- Shi JT, Hou CH, Wang S, Xiong XY, Wu SG, Liu C (2019) The semi-analytical productivity equations for vertically fractured coalbed methane wells considering pressure propagation process, variable mass flow, and fracture conductivity decrease. *J Petrol Sci Eng* 178:528–543. <https://doi.org/10.1016/j.petrol.2019.03.047>
- Sun Z, Shi JT, Wu KL, Zhang T, Feng D, Li XF (2019) Effect of pressure-propagation behavior on production performance: implication for advancing low-permeability coalbed-methane recovery. *SPE J* 24(02):681–697. <https://doi.org/10.2118/194021-PA>
- Talapatra A (2020) A study on the carbon dioxide injection into coal seam aiming at enhancing coal bed methane (ECBM) recovery. *J Petrol Explor Prod Technol* 10:1965–1981. <https://doi.org/10.1007/s13202-020-00847-y>
- Talapatra A, Karim MM (2020) The influence of moisture content on coal deformation and coal permeability during coalbed methane

- (CBM) production in wet reservoirs. *J Petrol Explor Prod Technol* 10:1907–1920. <https://doi.org/10.1007/s13202-020-00880-x>
- Uddin N, Blommerde M, Taplin R, Laurence D (2015) Sustainable development outcomes of coal mine methane clean development mechanism projects in China. *Renew Sust Energy Rev* 45:1–9. <https://doi.org/10.1016/j.rser.2015.01.053>
- Vishal V, Singh L, Pradhan SP, Singh TN, Ranjith PG (2013) Numerical modeling of Gondwana coal seams in India as coalbed methane reservoirs substituted for carbon dioxide sequestration. *Energy* 49:384–394. <https://doi.org/10.1016/j.energy.2012.09.045>
- Wang G, Qin Y, Xie YW, Shen J, Zhao L, Huang B, Zhao WQ (2018) Coalbed methane system potential evaluation and favourable area prediction of Gujiao blocks, Xishan coalfield, based on multi-level fuzzy mathematical analysis. *J Petrol Sci Eng* 160:136–151. <https://doi.org/10.1016/j.petrol.2017.10.042>
- Wei YC, Li C, Cao DY, Wang AM, Zhang AX, Yao Z (2019a) The effects of particle size and inorganic mineral content on fines migration in fracturing proppant during coalbed methane production. *J Petrol Sci Eng* 182:106355. <https://doi.org/10.1016/j.petrol.2019.106355>
- Wei Q, Li XQ, Hu BL, Zhang XQ, Zhang JZ, He YK, Zhang YC, Zhu WW (2019b) Reservoir characteristics and coalbed methane resource evaluation of deep-buried coals: A case study of the No. 13–1 coal seam from the Panji Deep Area in Huainan Coalfield, Southern North China. *J Petrol Sci Eng* 179:867–884. <https://doi.org/10.1016/j.petrol.2019.04.100>
- Wu Y, Liu JS, Elsworth D, Chen ZW, Connell L, Pan ZJ (2010) Dual poroelastic response of a coal seam to CO₂ injection. *Int J Greenh Gas Con* 4(4):668–678. <https://doi.org/10.1016/j.ijggc.2010.02.004>
- Xia TQ, Zhou FB, Gao F, Kang JH, Liu JD, Wang JG (2015) Simulation of coal self-heating processes in underground methane-rich coal seams. *Int J Coal Geol* 141:1–12. <https://doi.org/10.1016/j.coal.2015.02.007>
- Xiong P, Hu WS, Hu HX, Liu HL (2020) Mechanism of shear failure near fracture face during drainage process of CBM well. *J Petrol Explor Prod Technol* 10:3309–3317. <https://doi.org/10.1007/s13202-018-0467-y>
- Xu JZ, Zhai C, Ranjith PG, Sun Y, Qin L (2019) Petrological and ultrasonic velocity changes of coals caused by thermal cycling of liquid carbon dioxide in coalbed methane recovery. *Fuel* 249:15–26. <https://doi.org/10.1016/j.fuel.2019.03.089>
- Yan J, Lu YY, Zhong DL, Zou ZL, Li JB (2019) Enhanced methane recovery from low-concentration coalbed methane by gas hydrate formation in graphite nanofluids. *Energy* 180:728–736. <https://doi.org/10.1016/j.energy.2019.05.117>
- Yang RY, Huang ZW, Li GS, Sepehrnoori K, Lin Q, Cai CZ (2017) Integrity Testing of a Polyvinyl Chloride slotted liner for horizontal Coalbed-Methane wells. *SPE Drill Complet* 32(02):86–96. <https://doi.org/10.2118/185958-PA>
- Yang RY, Huang ZW, Yu W, Lashgari H, Sepehrnoori K (2018) A semianalytical method for modeling two-phase flow in coalbed-methane reservoirs with complex fracture networks. *SPE J*. <https://doi.org/10.15530/urtec-2016-2460741>
- Yu Y, Wang Y (2020) Characteristics of low-rank coal reservoir and exploration potential in Junggar Basin: new frontier of low-rank CBM exploration in China. *J Petrol Explor Prod Technol* 10:2207–2223. <https://doi.org/10.1007/s13202-020-00923-3>
- Zhang CL, Xu J, Peng SJ, Li QX, Yan FZ, Chen YX (2018) Dynamic behavior of gas pressure and optimization of borehole length in stress relaxation zone during coalbed methane production. *Fuel* 233:816–824. <https://doi.org/10.1016/j.fuel.2018.06.132>

Publisher's Note Springer Nature remains neutral with regard to jurisdictional claims in published maps and institutional affiliations.